Dielectric function and optical conductivity of TiO_x ($0.8 < x < 1.3$) determined from electron energy-loss spectroscopy

Shubha Gokhale*
Solid State and Structural Chemistry Unit, Indian Institute of Science, Bangalore 560 012, India and Jawaharlal Nehru Centre for Advanced Scientific Research, Indian Institute of Science, Bangalore 560 012, India

S. R. Barman
Solid State and Structural Chemistry Unit, Indian Institute of Science, Bangalore 560 012, India

D. D. Sarma†
Solid State and Structural Chemistry Unit, Indian Institute of Science, Bangalore 560 012, India and Jawaharlal Nehru Centre for Advanced Scientific Research, Indian Institute of Science, Bangalore 560 012, India
(Received 22 June 1995)

Reflection electron energy-loss spectra are reported for the family of compounds TiO_x over the entire homogeneity range ($0.8 < x < 1.3$). The spectra exhibit a plasmon feature on the low-energy side, while several interband transitions are prominent at higher energies. The real and imaginary parts of dielectric functions and optical conductivity for these compounds are determined using the Kramers-Kronig analysis. The results exhibit systematic behavior with varying oxygen stoichiometry.

I. INTRODUCTION

Titanium oxide has been a topic of interest for various investigations, due to its physical and chemical properties which are important from a technological point of view. Varying the oxygen content changes the conductivity of the sample from metallic (TiO) to a wide gap insulator (TiO_2). TiO_x can be formed homogeneously over a wide range of x ($0.8 < x < 1.3$) retaining the rocksalt structure of the monoxide TiO. There have been many attempts to experimentally and theoretically determine the electronic structure of TiO_x.[1–5] In contrast, there have been comparatively few attempts to find the optical properties of titanium oxide using different techniques. Plasma frequencies for different compositions of TiO_x (x=0.8, 1.0, and 1.2) have been determined[6] using reflectance spectroscopy. Subsequently, the dielectric functions of a clean titanium surface and oxidized titanium surface between 2 and 25 eV were obtained from reflectivity studies,[7] however, the exact stoichiometry of the oxide species present on the surface was not known in this case. Dielectric functions have also been obtained for nominal TiO and TiO_2 from an analysis of transmission electron energy-loss spectra.[8] While it is known that transport properties are pronouncedly affected by changing the oxygen content of TiO_x over the homogeneity range, there has been no attempt to determine the dielectric function or the optical conductivity of TiO_x with a systematic variation of oxygen stoichiometry. Here, we report a reflection electron energy-loss spectroscopy (REELS) investigation of TiO_x with such a variation of oxygen content over the entire homogeneity range ($0.8 < x < 1.3$). REEL spectra obtained consist of plasmon features at lower energies and interband transitions at higher energies. We interpret our results on the basis of band structure calculations carried out for this system.[3] We believe that the band approach to explain the origin of loss features observed in the REEL spectra is more appropriate in these broadband systems compared to earlier approaches[2,4,8] based on molecular orbital diagrams. Furthermore, we have determined the real and the imaginary parts of the dielectric function from Kramers-Kronig analysis of the spectra, corrected for multiple scattering effects. Both the components of dielectric functions show systematic variations with varying oxygen stoichiometry. Optical conductivities were obtained from the imaginary parts of the dielectric functions.

II. EXPERIMENT

TiO_x ($0.8 < x < 1.3$) samples were prepared by melt quenching a mixture of Ti and TiO_2 in the required proportions using an arc furnace under argon atmosphere. The oxygen stoichiometry (x) was determined by measuring the increase in the weight of samples on oxidation to TiO_2 at 1000 °C in flowing oxygen. The estimated compositions were found to be $TiO_{0.81}$, $TiO_{0.91}$, $TiO_{1.03}$, $TiO_{1.18}$, and $TiO_{1.30}$ corresponding to starting compositions of $TiO_{0.8}$, $TiO_{0.9}$, $TiO_{1.0}$, $TiO_{1.15}$, and $TiO_{1.28}$, respectively.

Reflection electron energy-loss spectroscopy measurements were carried out in a combined x-ray photoemission spectroscopy–ultraviolet photoemission spectroscopy–bremsstrahlung isochromat spectroscopy spectrometer from VSW Scientific Limited, U.K. The sample surface was cleaned by scraping with an alumina file in a vacuum of 5×10^{-10} mbar. The cleanliness of

0163-1829/95/52(20)/14526(5)/$06.00 ©1995 The American Physical Society

sample surfaces was checked by monitoring the O 1s and C 1s core levels with x-ray photoemission spectroscopy. REELS spectra were collected using a hemispherical analyzer with constant pass energy of 10 eV. The primary electron beam with 0.4 eV full width at half maximum (FWHM) of elastic peak was incident on the sample surface at 45° angle with respect to the sample normal. The REEL spectra were collected at normal emission with spectrometer energy resolution of 0.1 eV. Thus, the total resolution for spectra reported here was limited by the energy spread of the primary electron beam. Spectra were recorded over a wide range of energy (0 – 56 eV), including the elastic peak. The spectra were recorded at various primary energies, though only the results obtained with 1500 eV are presented here. At this energy, we expect a typical mean free path of about 20 Å, which makes it a rather surface sensitive probe. However, our recent comparison of photoemission results with bulk band structure calculations for these systems[3] suggests that the electronic structure is not greatly changed, due to surface effects in these systems.

III. DATA ANALYSIS

As recorded REELS spectra are dominated by the elastic peak. This peak was removed from the raw data and the spectrum was extrapolated to zero intensity at 0 eV loss energy by quadratic curve fit ($aE^2 + bE$) between 0 eV and about 1.5 eV, as was employed earlier in the case of metallic cuprates.[9] As this extrapolation is on a very narrow frequency interval, its effect on the final result is not very significant. Since the experimental spectra were recorded over a finite frequency range (0–56 eV), the loss intensity was assumed to have a dependence of ω^{-4} beyond the experimentally obtained range on the basis of free electron gas approximation.[10–12] This approximation does not significantly affect the results of subsequent analysis for energies less than about 50 eV. It is also known that the REEL spectra can have prominent features arising from surface plasmon excitations. We have, therefore, checked the REEL spectra from these compounds with various primary energies. With decreasing primary energy, the surface sensitivity can be increased, thereby identifying the surface related features. This way we have ensured that the spectral features obtained at 1500 eV have minimal contributions from surface plasmons and thus, have neglected any small contribution from this process in all data analysis. However, the spectra were corrected for multiple scattering effects, using an iterative procedure; the convergence criterion ensured that the total squared error between the results of two consecutive steps is less than 10^{-6} on convergence.

The resultant single scattering loss function, $S(E)$ was normalized with a factor C, where C is defined as

$$C = \frac{\pi}{2\int_0^\infty \frac{S(E')}{E'}dE'} .$$

This normalization procedure is consistent with the metallic ground state of these samples[12] and ensures that the real part of the inverse of the dielectric function [$\mathrm{Re}(1/\epsilon(E))$] vanishes at zero energy.

The normalized single scattering loss function [$= \mathrm{Im}(-1/\epsilon(E))$] thus obtained was used to determine the real part of inverse of the dielectric function, using the Kramers-Kronig analysis.[12]

$$\mathrm{Re}\frac{1}{\epsilon(E)} = 1 - \frac{2}{\pi}\mathrm{P}\int_0^\infty \frac{E'\mathrm{Im}\left(-\frac{1}{\epsilon(E')}\right)}{E'^2 - E^2}dE' ,$$

where P denotes the principal part of Cauchy's integral. The integral was calculated numerically. Subsequently, $\epsilon_1 = \mathrm{Re}(\epsilon)$ and $\epsilon_2 = \mathrm{Im}(\epsilon)$ were determined by

$$\epsilon_1(E) = \frac{\mathrm{Re}\left(\frac{1}{\epsilon(E)}\right)}{\left[\mathrm{Re}\left(\frac{1}{\epsilon(E)}\right)\right]^2 + \left[\mathrm{Im}\left(\frac{1}{\epsilon(E)}\right)\right]^2}$$

and

$$\epsilon_2(E) = \frac{\mathrm{Im}\left(-\frac{1}{\epsilon(E)}\right)}{\left[\mathrm{Re}\left(\frac{1}{\epsilon(E)}\right)\right]^2 + \left[\mathrm{Im}\left(\frac{1}{\epsilon(E)}\right)\right]^2} .$$

Using the imaginary part of the dielectric function, the optical conductivity was determined from

$$\sigma(\omega) = \frac{\epsilon_2(\omega) \times \omega}{4\pi} .$$

IV. RESULTS AND DISCUSSION

We show REEL spectra normalized to the elastic peak heights for TiO_x with different values of x in Fig. 1. All these spectra exhibit four prominent features at 2–4 eV, 13–14 eV, 25–26 eV, 47–49 eV and match qualitatively with the ones reported in Ref. 8 for nominal TiO using transmission-electron energy-loss spectroscopy (TEELS). The first loss feature appears at 3.9 eV in case of $TiO_{0.81}$ and shifts gradually towards lower energy with increasing oxygen content. For $TiO_{1.30}$, this feature is at 2.2 eV. This feature is attributed to a plasmon loss. Earlier studies reported a plasmon loss feature at about 3.8 eV for nominal $TiO_{1.0}$ and a reduction in plasmon frequency with increasing oxygen content.[6] The plasmon frequency is indeed expected to decrease with a decreasing number of conduction electrons. In the case of nearly free electrons, the plasmon frequency ω_p is given by

$$\omega_p^2 = \frac{4\pi n e^2}{m^*} ,$$

where n is the number of electrons and m^* is the effective mass. The number n of d electrons available in TiO_x is given by $n = 4 - 2x$. We find that while ω_p^2 exhibits the expected monotonic increase with n, the dependence differs considerably from the expected linear

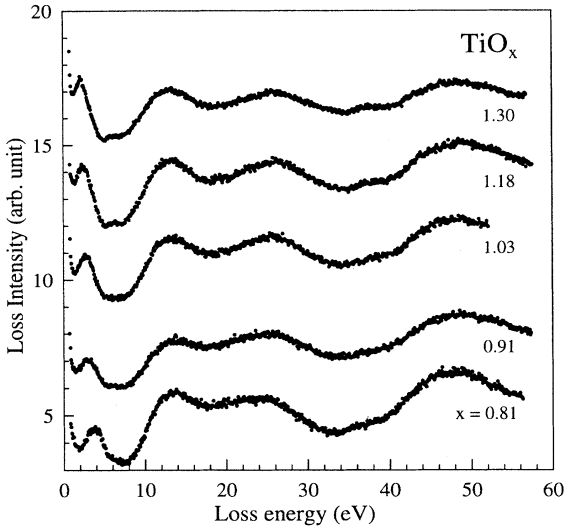

FIG. 1. Electron energy-loss spectra of TiO_x for various values of x, normalized to the elastic peak (not shown). The spectra have been shifted along the y axis for clarity by the following amounts: 0.0 ($x = 0.81$), 4.0 ($x = 0.91$), 7.0 ($x = 1.03$), 10.0 ($x = 1.18$), and 14.0 ($x = 1.30$).

behavior arising from the uncertainties in determining the peak positions.

Higher energy-loss features arise from various interband transitions. In order to interpret these features, we report in Fig. 2(a) the total density of states (DOS) and a few specific partial DOS of vacancy ordered TiO, using linearized muffin tin orbital method (LMTO). It has been shown earlier[3] that these band structure results provide a realistic description of the electronic structure of these compounds. While for the common range of energies, the DOS shown in Fig. 2(a) is similar to that in Ref. 3, Fig. 2(a) presents the results over a wider energy range along with different partial DOS, relevant to the present discussion.

While band structure results, in terms of DOS and various partial DOS could be directly compared to photoemission and inverse photoemission spectra,[3] EEL spectra correspond to transitions between the occupied and the unoccupied bands and thus cannot be directly compared to the DOS. However, if we assume that dipole transitions dominate the EEL spectra at the primary energy used here and that transition matrix elements do not depend very much on the loss energy, individual dipole allowed channels ($S_{l\to l\pm1}(\epsilon)$) will contribute to the total EEL spectrum in the following way:

$$S_{l\to l\pm1}(\epsilon) \propto \int_{E_F-\epsilon}^{E_F} \rho_l(\epsilon')\rho_{l\pm1}(\epsilon'+\epsilon)d\epsilon' ,$$

where ρ_l and $\rho_{l\pm1}$ represent the partial density of states corresponding to l and $(l \pm 1)$ angular momentum components, respectively. Due to the specific limits of integration here, ρ_l spans the occupied part of the partial DOS and $\rho_{l\pm1}$ is only over the unoccupied parts; thus, $S_{l\to l\pm1}(\epsilon)$ represent various joint densities of states. The total EEL spectrum consists of a transition probability-weighted average of $S_{l\to l\pm1}(\epsilon)$ for all angular momenta, l. While we cannot calculate transition probabilities for different $l \to l \pm 1$ channels and thus cannot obtain a quantitative theoretical description of the EEL spectra, it is to be noted that qualitative features in the EEL spectrum (such as peak positions) must reflect in similar features in the individual $S_{l\to l\pm1}(\epsilon)$. Thus, we have calculated these angular momentum specific joint densities of states for different l's and the results are shown for Ti $p \to d$, O $p \to s$ and $p \to d$ transitions in Fig. 2(b), since only these appear to have significant intensities. In order to compare these results with the experimental ones, we have expanded the energy axis by a factor of 1.3 in Fig. 2(b). This is necessitated by the fact that the local density approximation calculation tends to underestimate energies of the unoccupied states; this is clearly evidenced in the comparison of unoccupied calculated DOS

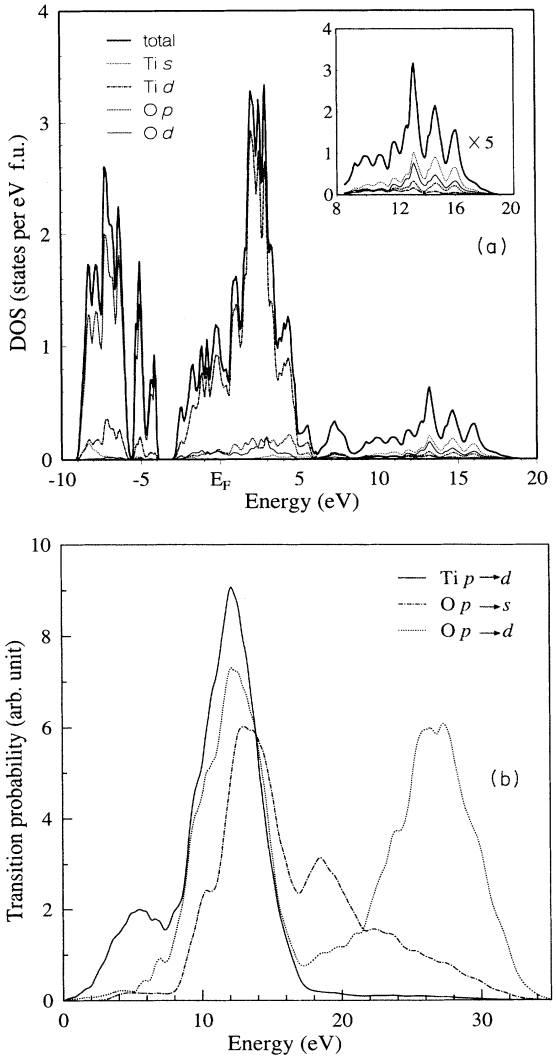

FIG. 2. (a) Total and some selected partial densities of states in TiO obtained from LMTO calculations. (b) Transition probabilities for dipolar excitations for selected channels in TiO calculated within an approximate scheme (see text) on the basis of the results shown in (a).

with the bremsstrahlung isochromat (BI) spectra of TiO_x presented in Ref. 3. With this single adjustable parameter to expand the energy axis, we find that the calculated results in Fig. 2(b) provide a very good description for the experimentally observed features. For example, all the three transitions, namely, Ti $p \rightarrow d$, O $p \rightarrow s$, and O $p \rightarrow d$, exhibit prominent feature around 13 eV corresponding to the experimentally observed EELS feature at about the same loss energy. Even the weaker features in the calculated results at about 5.5 and 18.5 eV may have weak corresponding features in some of the experimental spectra shown in Fig. 1 at about the same energy, arising from primarily Ti $p \rightarrow d$ and O $p \rightarrow s$ transitions, respectively. Similarly, a comparision of EELS data in Fig. 1 and the calculated plots in Fig. 2(b) suggest that the second prominent experimental feature at about 26 eV arises from an oxygen $p \rightarrow d$ interband transition. This interpretation is in contrast to the assignment of this peak in Ref. 8 to a collective excitation of the total valence electrons. However, there can be a contribution to this loss feature from excitations of oxygen $2s$ electrons to oxygen p states just above the Fermi energy. It is interesting to note that there appears to be a systematic variation in the energy position of this loss feature with changing oxygen content in TiO_x; thus, the peak appears at about 24.5 eV for $TiO_{0.81}$ and at about 26 eV for $TiO_{1.3}$. Since no major changes are observed in x-ray photoemission and BI spectra of these compounds,[3] these small changes may indicate minor rearrangements of the unoccupied oxygen p partial density of states with changing oxygen content.

The fourth feature is in the form of a very broad hump centered around 48 eV. This feature is accompanied by a shoulder at about 37 eV, which is more prominent for samples with higher oxygen contents. These high energy-loss features cannot be explained on the basis of the calculation of joint density of states presented in Fig. 2(b). The main feature at 48 eV is possibly due to electronic transitions from the Ti $3p$ to unoccupied Ti $3d$ level. The origin of the shoulder, however, remains unclear.

In Figs. 3 and 4, we show the real (ϵ_1) and the imaginary (ϵ_2) parts of the dielectric function over a wide energy range for these compounds obtained by the Kramers-Kronig analysis of loss functions shown in Fig. 1. Overall shapes of ϵ_1 and ϵ_2 are very similar for different compounds in this series.

The $\epsilon_1(\omega)$ curves are mainly dominated by a peak at about 7 eV. At higher energies, there are broad features appearing at about 18 eV, 35 eV, and 41 eV. These high energy features arise due to interband transitions as discussed above in detail. The value of ϵ_1 at 7 eV systematically increases from 1.5 for $TiO_{0.81}$ to 1.85 in case of $TiO_{1.30}$, while the other features have almost the same intensity for different compositions. The imaginary part of dielectric function, ϵ_2 represents the dissipative part. The $\epsilon_2(\omega)$ curves (Fig. 4) show the first feature at about 10 eV. At higher energy, two broad features appear at about 21 eV and 43 eV. The amplitude of the peak at 10 eV decreases from 1.5 for $TiO_{0.81}$ to 1.15 for $TiO_{1.30}$. The amplitude of the remaining features remains more or less constant over the entire range of oxygen content.

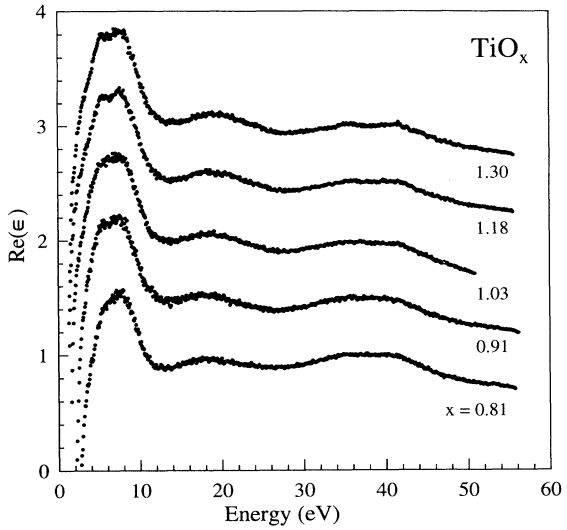

FIG. 3. Real parts of the dielectric functions for TiO_x for various values of x. The plots have been shifted along the y axis for clarity by the following amounts: 0.0 ($x = 0.81$), 0.5 ($x = 0.91$), 1.0 ($x = 1.03$), 1.5 ($x = 1.18$), and 2.0 ($x = 1.30$).

The positions of the features reported here are in agreement with the results obtained from reflectivity spectra by Wall *et al.* in case of an oxidized surface, which they identify as TiO.[7]

Figure 5 depicts the optical conductivity $\sigma(\omega)$ of these samples as a function of energy. Prominent features in these plots appear at about 3 eV, 10 eV, 23 eV, and 45 eV. The low intensity feature at about 3 eV closely matches in energy to the feature in EEL spectra (Fig. 1) attributed to a plasmon loss. Furthermore, this feature in $\sigma(\omega)$ shows a systematic shift to lower energy

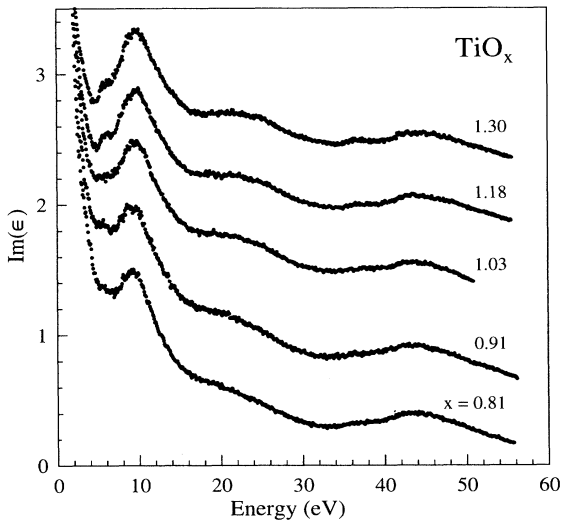

FIG. 4. Imaginary parts of the dielectric functions for TiO_x for various values of x. The plots have been shifted along the y axis for clarity by the following amounts: 0.0 ($x = 0.81$), 0.5 ($x = 0.91$), 1.2 ($x = 1.03$), 1.7 ($x = 1.18$), and 2.2 ($x = 1.30$).

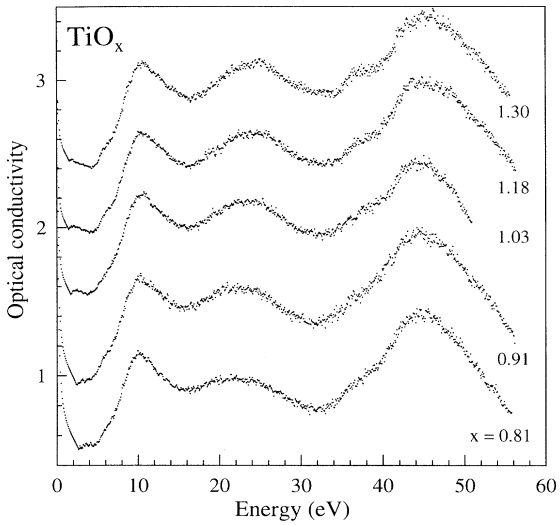

FIG. 5. Optical conductivities of TiO_x for various values of x. The plots have been shifted along the y axis for clarity by the following amounts: 0.0 ($x = 0.81$), 0.5 ($x = 0.91$), 1.2 ($x = 1.03$), 1.7 ($x = 1.18$), and 2.2 ($x = 1.30$).

with increasing oxygen content in the sample, which is the same behavior as in the case of the plasmon loss feature in EEL spectra. The pronounced peak in $\sigma(\omega)$ at about 10 eV most probably arises from oxygen p to titanium d transition, the energy difference between these bands [Fig. 2(a)] being in good agreement with the energy of this feature. The feature near 23 eV can be attributed to oxygen p–oxygen d excitations [Fig. 2(b)] and to oxygen $2s$–Ti d and oxygen p admixed states just above E_F. The higher energy features in $\sigma(E)$ at about 37 eV and 45 eV probably arise from Ti $3p$ core excitations. Though the value of conductivity remains almost unaltered between different samples on the higher-energy side, the first feature at 3 eV shows a decrease in intensity with increasing oxygen content. This trend is similar to that of dc conductivities reported by Banus *et al.* for TiO_x ($0.86 < x < 1.17$).[13] Hence at lower energies, where the free electrons in the system govern the data, there is a systematic change observed in the conductivity. At higher energies, where the interband transitions dominate the loss spectrum, the conductivity remains almost unaltered with oxygen content.

In conclusion, we have presented electron energy-loss spectra of TiO_x for five compositions with $0.81 \leq x \leq 1.3$. Various features in the spectra have been interpreted with the help of *ab initio* band structure calculations. Real and imaginary parts of the complex dielectric function have been obtained from the loss spectra by Kramers-Kronig analysis; optical conductivity of the samples have been calculated from the dielectric function. The low-energy part of the optical conductivity is found to decrease systematically with increasing oxygen content in the samples similar to dc conductivity results.

ACKNOWLEDGMENTS

We thank Professor C.N.R. Rao for his continued support. Support for this work from the Homi Bhabha Fellowship Council and the Department of Science and Technology, Government of India, is gratefully acknowledged. S.R.B. is thankful for support from the Council for Scientific and Industrial Research, Government of India.

* Present address: Physik Department E-20, Technische Universitat Munchen, D 85747 Garching, Germany.
† Electronic address: sarma@sscu.iisc.ernet.in

[1] J.M. Schoen and S.P. Denker, Phys. Rev. **184**, 864 (1969).
[2] D.W. Fischer, J. Appl. Phys. **41**, 3561 (1970).
[3] S.R. Barman and D.D. Sarma, Phys. Rev. B **49**, 16 141 (1994).
[4] K. Tsutsumi, O. Aita, and K. Ichikawa, Phys. Rev. B **15**, 4638 (1977).
[5] J.B. Goodenough, Phys. Rev. B **5**, 2764 (1972).
[6] C.N.R. Rao, W.E. Wahnsiedlser, and J.H. Honig, J. Solid State Chem. **2**, 315 (1970).
[7] W.E. Wall, M.W. Ribarsky, and J.R. Stevenson, J. Appl. Phys. **51**, 661 (1980).
[8] J. Frandon, B. Brousseau, and F. Pradal, J. Phys. **39**, 839 (1979).
[9] J. Yuan, L.M. Brown, and W.Y. Liang, J. Phys. C **21**, 517 (1988).
[10] H. Ibach and D.L. Mills, in *Electron Energy Loss Spectroscopy and Surface Vibrations* (Academic Press, New York, 1982).
[11] H. Raether, in *Excitation of Plasmons and Interband Transitions by Electrons*, Springer Tracts in Modern Physics Vol. 88 (Springer-Verlag, Berlin, 1980); *Springer Tracts in Modern Physics* (Springer-Verlag, Berlin, 1965), Vol. 38, p. 85.
[12] J. Daniels, C.V. Festenberg, H. Raether and K. Zeppenfeld, *Springer Tracts in Modern Physics* (Springer-Verlag, Berlin, 1970) Vol. 54, p. 77.
[13] M.D. Banus, T.B. Reed, and A.J. Strauss, Phys. Rev. B **5**, 2775 (1972).